Comparison of functional parcellation embedding quality on resting-state fMRI in heterogeneous data

Désirée Lussier[a,b], AmanPreet Badhwar[a,c], Amal Boukhdhir[d], François Paugam[d], Hanad Shamarke[a], Simon Duchesne[e,f], Pierre Bellec[a,b]

a Centre de recherche de l'Institut universitaire de gériatrie de Montréal, Montréal, QC, Canada; b Psychology Department, Université de Montréal, Montréal, QC, Canada; c Department of Pharmacology and Physiology, Faculty of Medicine, Université de Montréal, Montréal, QC, Canada; d Département d'informatique et de recherche opérationnelle, Université de Montréal, Montréal, QC, Canada; e Département de radiologie, Faculté de médicine, Université Laval, Québec, Canada; f Centre CERVO, Institut universitaire en santé mentale de Québec, Québec, Canada

Introduction

Background: Soft parcels, generated through dictionary learning, have been shown to outperform hard parcels in terms of homogeneity[1] and homogeneity is limited in many current fMRI parcellation techniques[2]. This is important as systematic bias in homogeneity would create artificial differences in connectivity. Dynamic parcellations can generate highly reproducible seed-based brain parcels[3]. Extending this work, Dynamic Parcel Aggregation with Clustering (Dypac)[4] is a python package capable of detecting stable whole-brain soft parcellations in fMRI data using a simple two-level clustering algorithm.

Aim: to compare Dypac with other commonly used functional parcellation atlases in terms of functional homogeneity on multiple large rsfMRI public datasets.

Hypothesis: Dypac embedding quality will be an improvement over other functional parcellation atlases of similar resolution.

Methods

Datasets: Single subject, multi-site dataset (SIMON, n = 72 scans), multi-subject, multi-side datasets (ADNI, n = 503; ABIDE, n = 760; ADHD200, n = 527; CCNA, n = 142; and CIMAQ, n = 95) with ~70% for training (n = 1610) and ~30% for test (n = 489)

Dypac models: 64 clusters and 512 states, 128 clusters and 512 states, 128 clusters and 1024 states, and 256 clusters and 1024 states, each run at 8mm and 5mm of smoothing

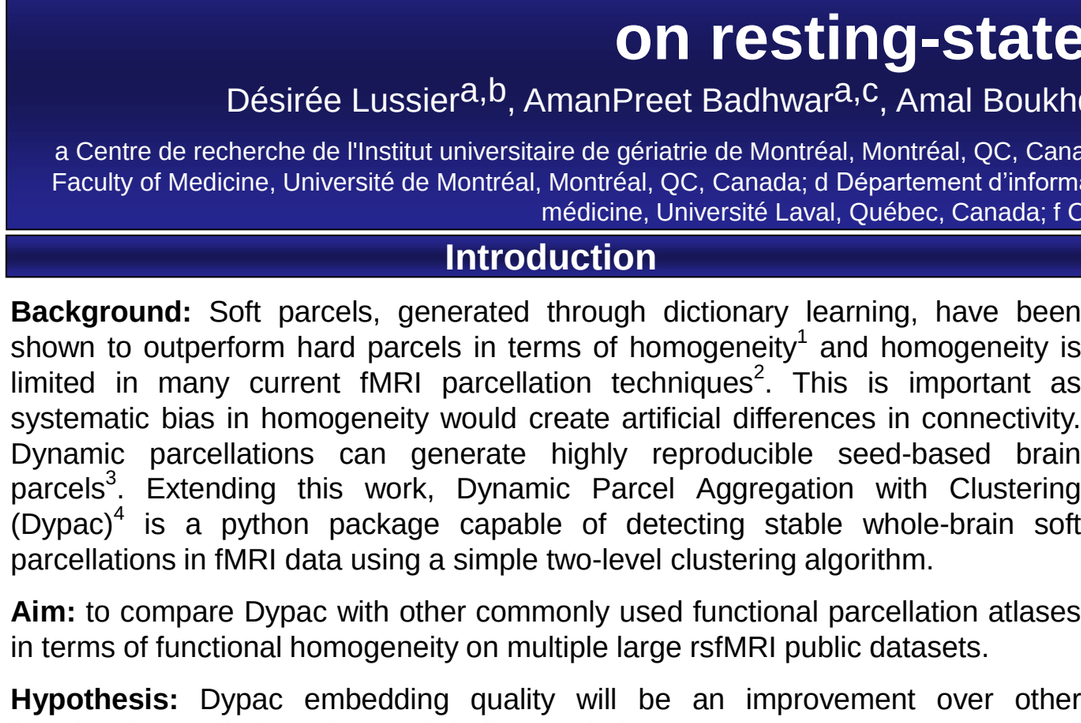

Figure 1 (above): For the first level of Dypac, k means is run directly on the time series using sliding time windows. This generates a family of parcels, which are represented with one-hot encoders. The second-level performs clustering on indicator functions of parcels aggregated over many windows. This procedure gives the stable maps.

R^2 maps: generated from individual time series, and used to quantify embedding quality, from each model resolution for each of the atlases:

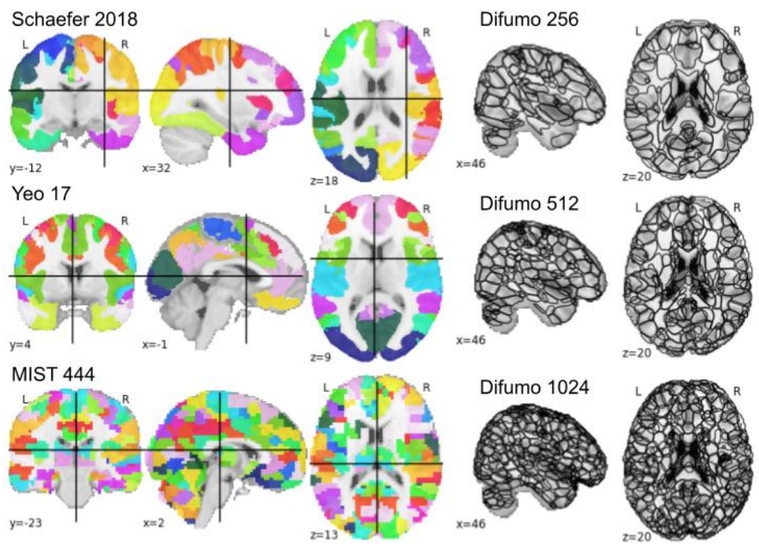

Figure 2 (above): Atlases used in the analyses: Dypac (at model resolutions; not depicted), Schaefer[6] (400 regions of interest), Yeo[7] (17 networks), MIST[8] (444), Smith[9] (70-dimensional ICA rsfMRI components; not depicted), Difumo[10] (256, 512, and 1024 dimensionalities)

Statistical analyses: Nistats[11] used to compare R^2 maps for significant differences in embedding quality between Dypac and other atlases, with α of 0.05 and FDR correction applied to each comparison. Nilearn math_img was used to compute the average of the R^2 maps at each resolution for each atlas.

Results

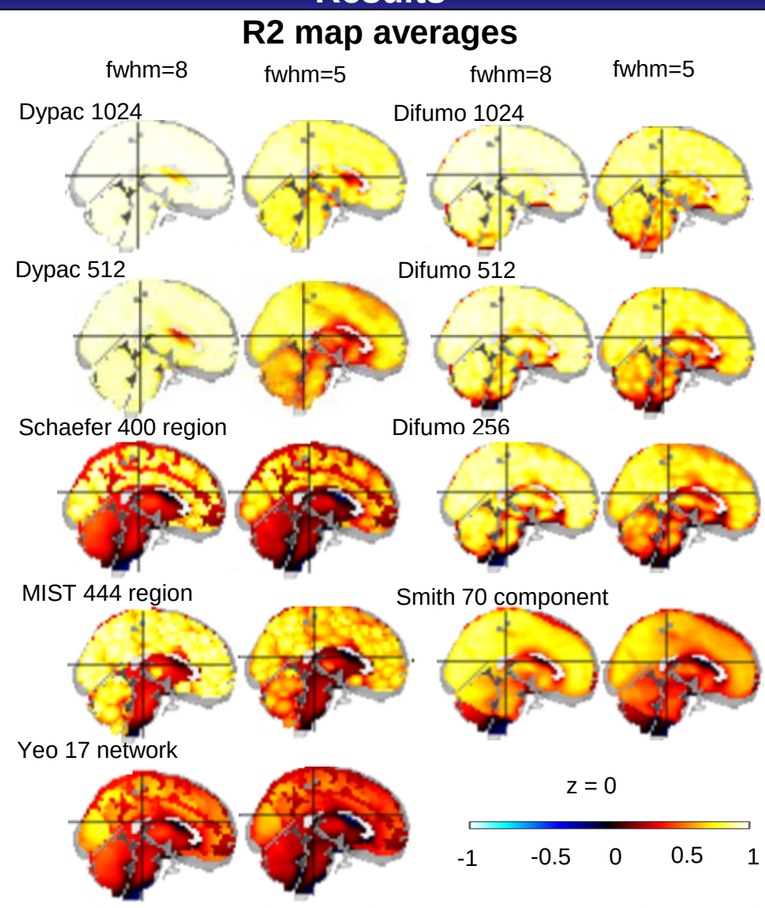

Figure 3 (above): Averaged R2 maps for Dypac 256 clusters and 1024 states, Dypac 64 clusters and 512 states, and for each of the atlases used in the analyses shown at the model resolution of 256 clusters and 1024 states at two different levels of smoothing. The columns represent the level of fwhm smoothing from which the embedding quality was derived where columns: 8mm (fwhm=8) and 5mm (fwhm=5). Positive values are depicted with warm colours (red, yellow) while negative values are depicted in cool colours (indigo, blue). These values are representative of embedding quality where a score of 1 is a perfect approximation, 0 is none, and negative is very poor.

- Overall embedding quality was higher for soft parcellations versus hard parcellations
- Both hard and soft parcellations embedding quality was greater for higher resolutions than lower
- Highest embedding quality was seen in Dypac and Difumo
- Smoothing but not model resolution impacted atlas performance for all but Dypac where both smoothing and model resolution had an impact

Comparisons of embedding quality between Dypac and Difumo

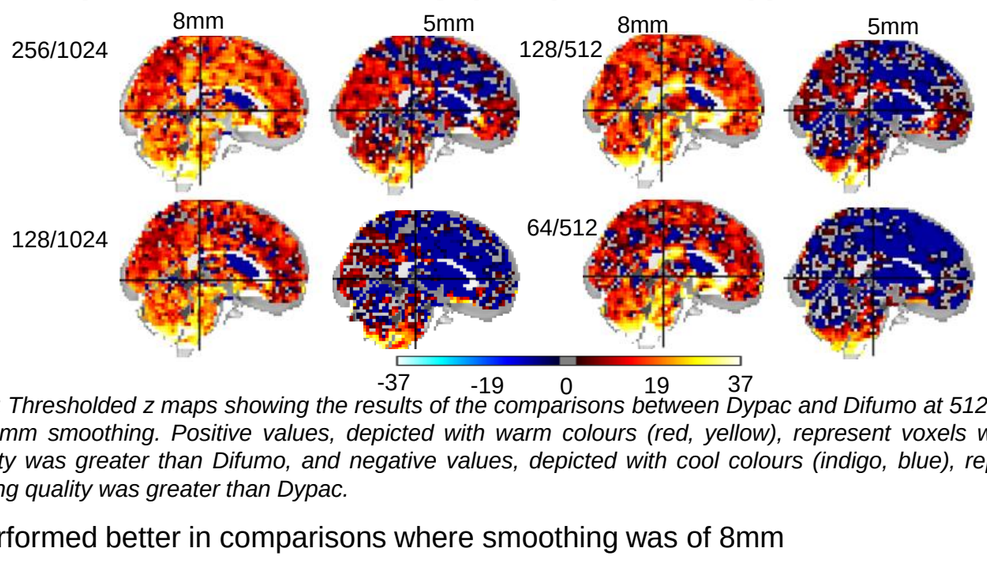

Figure 4 (above): Thresholded z maps showing the results of the comparisons between Dypac and Difumo at 512 and 1024 resolutions with 8mm and 5mm smoothing. Positive values, depicted with warm colours (red, yellow), represent voxels where average Dypac embedding quality was greater than Difumo, and negative values, depicted with cool colours (indigo, blue), represent voxels where Difumo embedding quality was greater than Dypac.

- Dypac performed better in comparisons where smoothing was of 8mm
- Difumo performed better for those with a smoothing of 5mm

Conclusion

Summary: Dypac embedding quality was an improvement over classic "hard" parcellations (Schaefer400, Yeo17, MIST444) as well as some low dimensional "soft" parcels (Smith ICA and Difumo256). Both Dypac and Difumo captured the majority of variance even with fairly low dimensions. Dypac works best for higher smoothing, Difumo works best for lower smoothing.

Limitations: Atlases were not all at the exact same resolution, which may bias homogeneity results. The hard atlas masks did not cover certain areas, such as the subcortical regions or cerebellum, and thus could not be properly compared on a whole brain analysis.

Future directions: Important areas for future exploration are the effects of Dypac hyper-parameters, whether dynamic hard parcels match (or exceed) the homogeneity of dictionary learning parcels, and if data generated at different sites (within studies) and populations (e.g. between studies) embed equally well.

Broader impact: These findings highlight the importance of atlas selection for compressing fMRI data, as well as the excellent performance of sparse dictionary learning with Dypac and Difumo.

References

1 Dadi, K., Varoquaux, G., Machlouzarides-Shalit, A., Gorgolewski, K., Wassermann, D., Thirion, B., & Mensch, A. (2020). Fine-grain atlases of functional modes for fMRI analysis. NeuroImage, (221), 117126. https://doi.org/10.1016/j.neuroimage.2020.117126
2 Urchs, S., Armoza, J., Moreau, C., Benhajali, Y., St-Aubin, J., Orban, P., & Bellec, P. (2019). MIST: A multi-resolution parcellation of functional brain networks. MNI Open Research, 1, 3. https://doi.org/10.12688/mniopenres.12767.2
3 Boukhdhir, A., Zhang, Y., Mignotte, M., & Bellec, P. (2021). Unraveling reproducible dynamic states of individual brain functional parcellation. Network Neuroscience, 1-41. https://doi.org/10.1162/netn_a_00168
4 https://github.com/courtois-neuromod/dypac
5 Bellec, P., Carbonell, F. M. , Perlbarg, V., Lepage, C., Lyttelton, O., Fonov, V., Janke, A., Tohka, J., Evans, A. (2011). A neuroimaging analysis kit for Matlab and Octave. Proceedings of the 17th International Conference on Functional Mapping of the Human Brain. https://niak.simexp-lab.org/build/html/PREPROCESSING.html
6 Schaefer, A., Kong, R., Gordon, E. M., Laumann, T. O., Zuo, X. N., Holmes, A. J., ... & Yeo, B. T. (2018). Local-global parcellation of the human cerebral cortex from intrinsic functional connectivity MRI. Cerebral cortex, 28(9), 3095-3114. https://doi.org/10.1073/pnas.0905267106
7 Yeo, B. T., Krienen, F. M., Sepulcre, J., Sabuncu, M. R., Lashkari, D., Hollinshead, M., ... & Buckner, R. L. (2011). The organization of the human cerebral cortex estimated by intrinsic functional connectivity. Journal of neurophysiology. https://dx.doi.org/10.1152%2Fjn.00338.2011
8 Urchs, S., Armoza, J., Moreau, C., Benhajali, Y., St-Aubin, J., Orban, P., & Bellec, P. (2019). MIST: A multi-resolution parcellation of functional brain networks. MNI Open Research, 1, 3. https://doi.org/10.12688/mniopenres.12767.2
9 Smith, S. M., Fox, P. T., Miller, K. L., Glahn, D. C., Fox, P. M., Mackay, C. E., ... & Beckmann, C. F. (2009). Correspondence of the brain's functional architecture during activation and rest. Proceedings of the national academy of sciences, 106(31), 13040-13045. https://doi.org/10.1073/pnas.0905267106
10 Dadi, K., Varoquaux, G., Machlouzarides-Shalit, A., Gorgolewski, KJ., Wassermann, D., Thirion, B., Mensch, A. (2020) Fine-grain atlases of functional modes for fMRI analysis. NeuroImage, Elsevier, pp.117126. https://doi.org/10.1016/j.neuroimage.2020.117126
11 Abraham, A., Pedregosa, F., Eickenberg, M., Gervais, P., Mueller, A., Kossaifi, J., ... & Varoquaux, G. (2014). Machine learning for neuroimaging with scikit-learn. Frontiers in neuroinformatics, 8, 14. https://doi.org/10.3389/fninf.2014.00014

Contact: desiree.Lussier.levesque@criugm.qc.ca; **Research supported by**

CCNA Canadian Consortium on Neurodegeneration in Aging
CCNV Consortium canadien en neurodégénérescence associée au vieillissement
CIMA-Q
Centre de recherche iugm Institut universitaire de gériatrie de Montréal
Université de Montréal
UNIQUE CENTRE
NEUROMOD THE COURTOIS PROJECT ON NEURONAL MODELLING